

Supporting Information

Modulation of the binding sites for an adaptable DNA interactive probe: efficient chromofluorogenic recognition of Al³⁺ and live cell bioimaging

Atanu Maji, Debarpan Mitra, Amitav Biswas, Moumita Ghosh, Rahul Naskar, Saswati Gharami, Nabendu Murmu and Tapan K. Mondal*

[†]*Department of Chemistry, Jadavpur University, Kolkata- 700032, India. E-mail: tapank.mondal@jadavpuruniversity.in*

[‡]*Department of Signal Transduction and Biogenesis Amines (STBA), Chittaranjan National Cancer Institute, Kolkata- 700026, India. E-mail: nabendu.murmu@cnci.org.in*

CONTENTS

Fig. S1: ¹H-NMR spectrum of HMCP

Fig. S2: ¹³C-NMR spectra of HMCP

Fig. S3: ESI mass spectra of HMCP

Fig.S4: ¹H-NMR spectrum of MCMP

Fig. S5: ¹³C-NMR spectra of MCMP

Fig. S6: ESI mass spectra of MCMP

Fig.S7: ¹H-NMR spectrum of MCMB

Fig. S8: ¹³C-NMR spectra of MCMB

Fig. S9: ESI mass spectra of MCMB

Fig. S10: Change in UV-Vis spectra of the MCMP (10 μM) and MCMB upon gradual addition of 2 equivalent of Al³⁺ (10 μM)

Fig. S11: Change in emission spectra of the the MCMP (10 μM) and MCMB upon gradual addition of 2 equivalent of Al³⁺ (10 μM)

Figure S12: Change in emission intensity of HMCP (10 μM) upon addition of different metal ions (40 μM) in MeOH at pH=7.2

Table. S1: Comparison of fluorescence intensity enhancement of HMCP and its analogues (10 μM) upon addition of Al³⁺ (20 μM).

Fig. S13: Linear response curve of HMCP depending on Al³⁺ concentration

Fig. S14: Binding constant curve of HMCP depending on Al³⁺ concentration from fluorescence titration data

Fig. S15: Lifetime decay profile of HMCP and HMCP-Al³⁺

Fig. S16: Bar diagram illustration of the relative emission intensity of HMCP upon addition of various metals (10 μM) in MeOH and Al³⁺ (20 μM) in presence of other metal ions.

Fig. S17: Fluorescence ‘OFF-ON-OFF’ repetitive cycle upon each sequential addition of Al³⁺ and EDTA

Fig. S18: Job’s plot of HMCP for Al³⁺

Table S2: Comparison of emission intensity enhancement of HMCP and its analogues upon addition of ct-DNA

Table S3: Recovery experiment for various natural water samples using the proposed methods

Fig. S19: IC₅₀ dose of the probe (HMCP) in human breast cancer cells

Table S4: Determination of emission quantum yield (Φ) of HMCP and its complex with Al³⁺

Fig. S20: pH study of HMCP for Al³⁺

Fig. S21: HRMS of HMCP-Al³⁺ complex

Fig. S22: Photosensitivity study of HMCP and its complex

Fig. S23: Determination of binding constant of HMCP depending on ct-DNA concentration using Benesi-Hildebrand equation

Fig. S24: Optimized structure of HMCP calculated by DFT/B3LYP/6-31+G(d) method

Fig. S25: Optimized structure of HMCP-Al³⁺ calculated by DFT/B3LYP/6-31+G(d) method

Fig. S26: Contour plots of some selected molecular orbitals of HMCP

Fig. S27: Contour plots of some selected molecular orbitals of HMCP-Al³⁺

Table S5. Energy and compositions of some selected molecular orbitals of HMCP - Al³⁺

Table S6. Vertical electronic transitions calculated by TDDFT/B3LYP/CPCM method for HMCP and HMCP-Al³⁺ in methanol

Fig. S28: Solvent optimization: Emission intensity change and fluorescence image of HMCP in different solvents in presence of Al³⁺

Table S7: Comparison of sensor HMCP with other previously reported probes with respect to testing condition LOD value and test strips experiment.

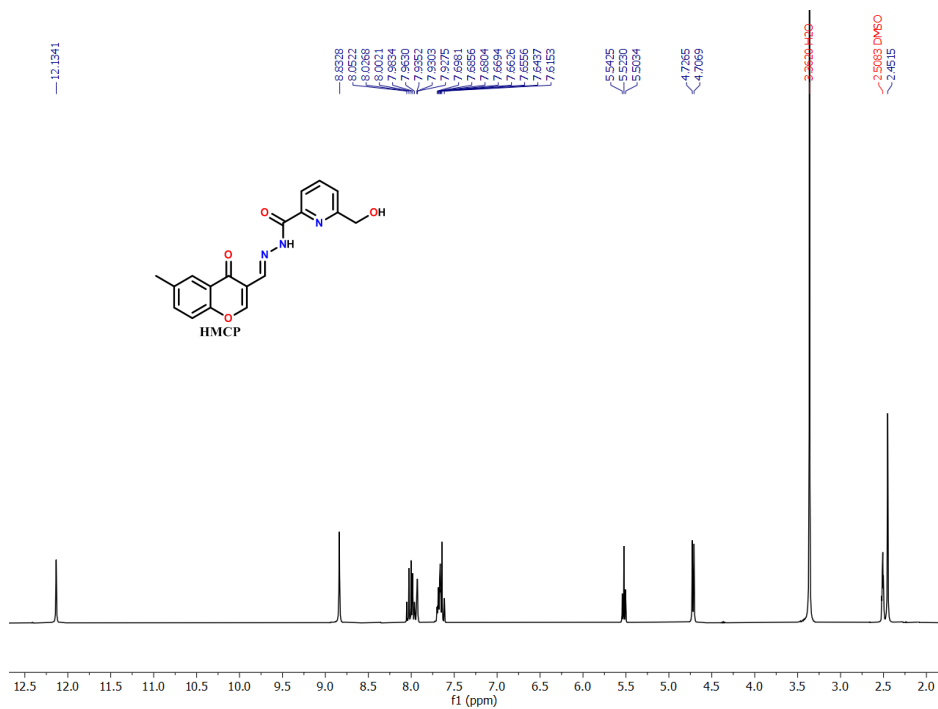


Figure S1: $^1\text{H NMR}$ (300 MHz) spectra of the probe (HMCP) in DMSO-d_6

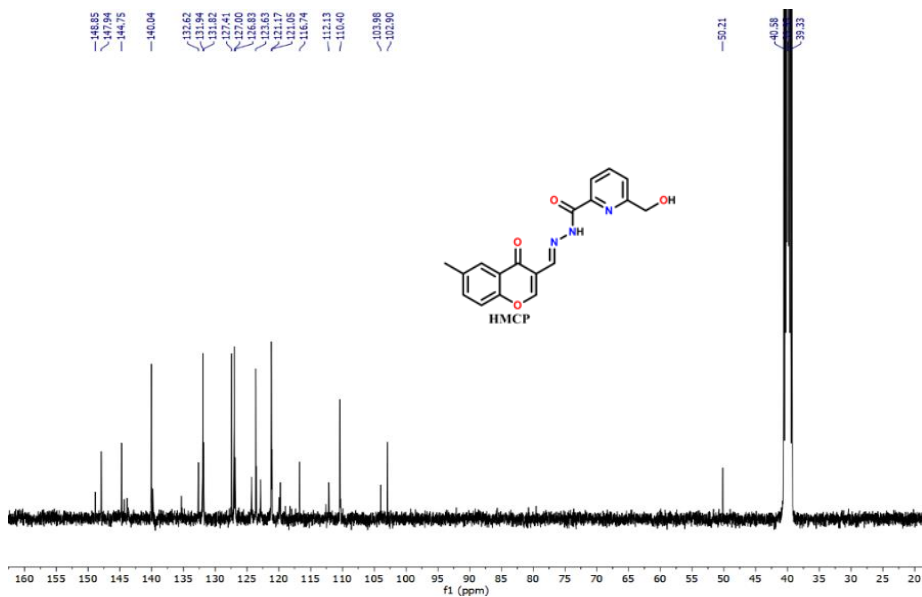


Figure S2: $^{13}\text{C NMR}$ (75 MHz) spectra of the probe (HMCP) in DMSO-d_6

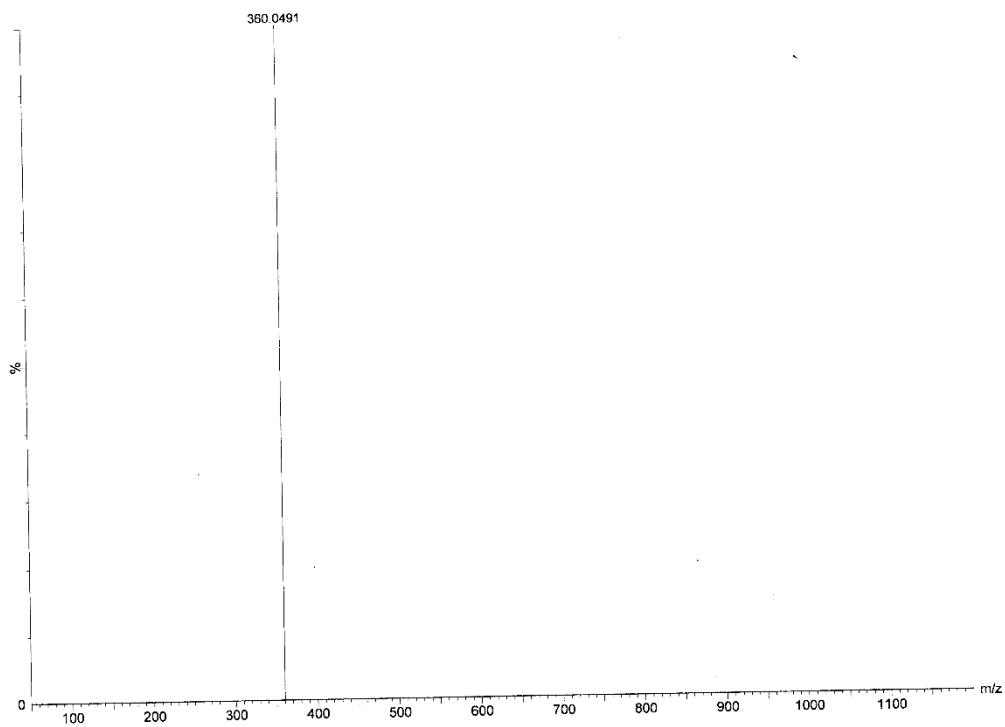


Figure S3: HRMS of the probe (HMCP)

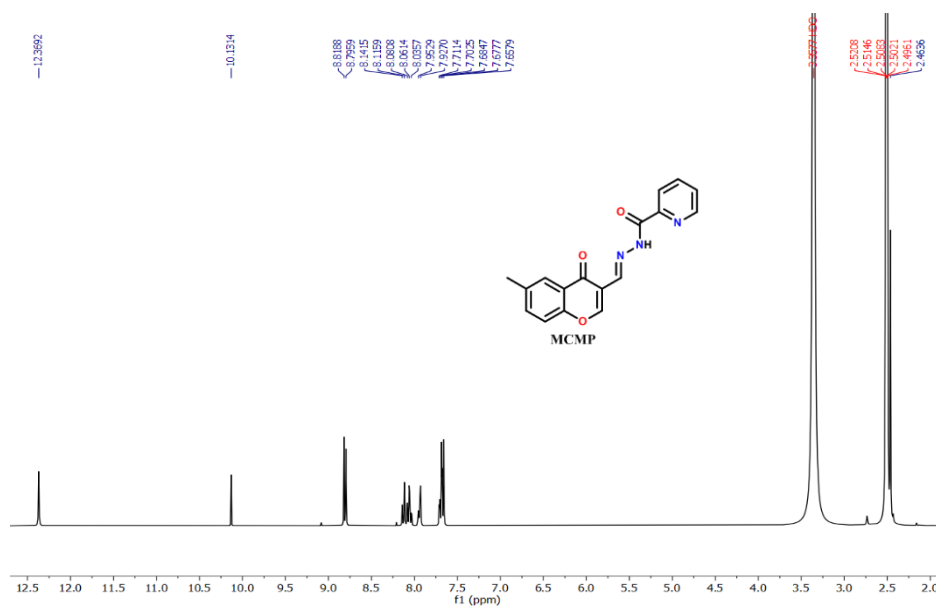


Figure S4: ¹H NMR (300 MHz) spectra of the probe (MCMP) in DMSO-d₆

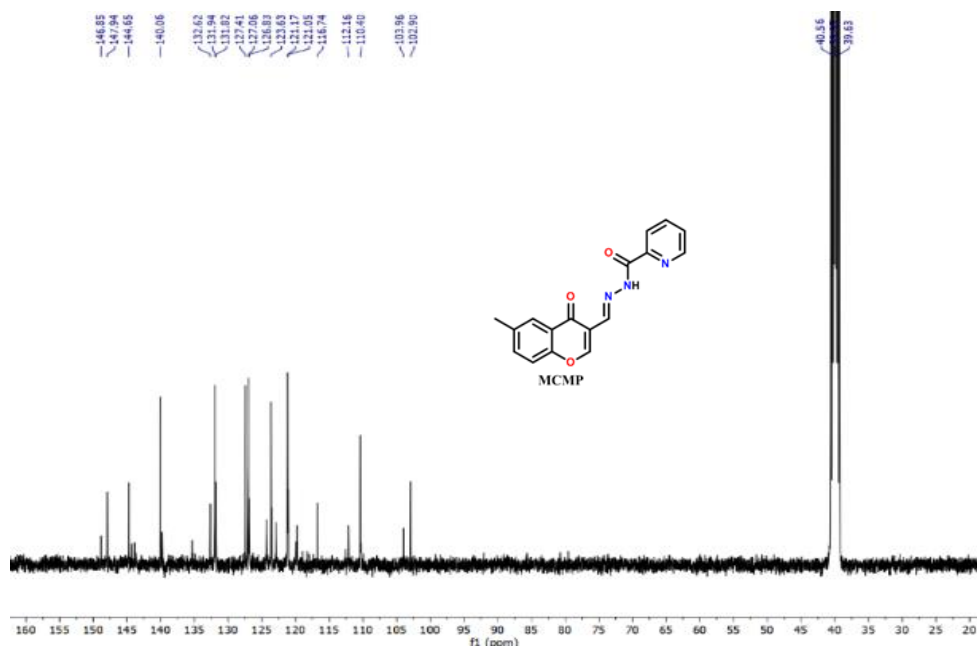


Figure S5: ¹³C NMR (75 MHz) spectra of the probe (MCMP) in DMSO-d₆

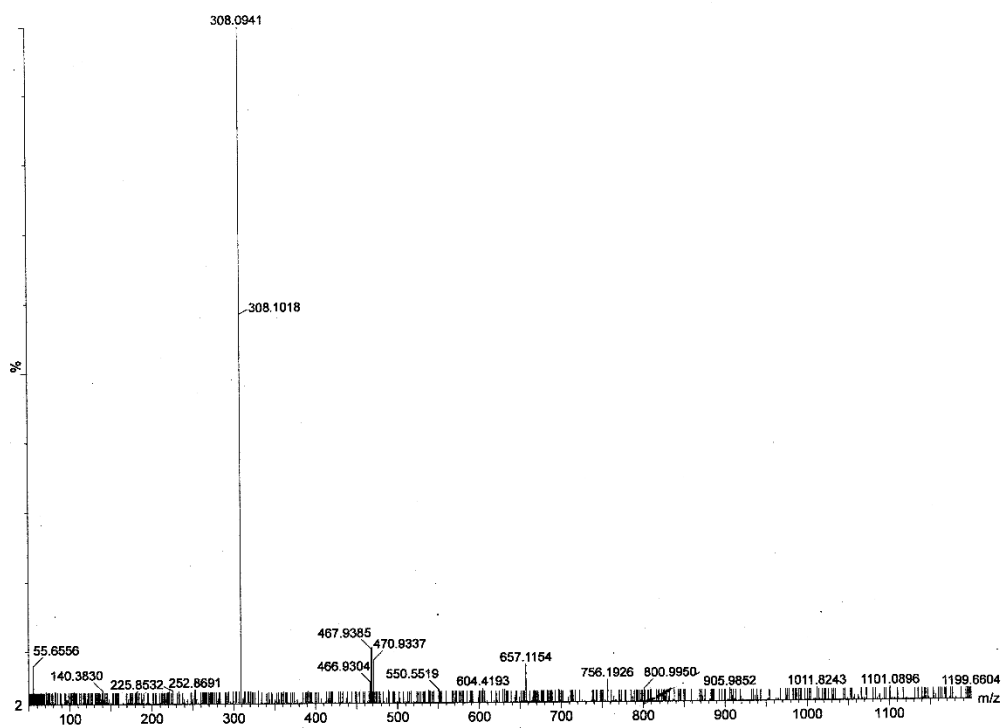


Figure S6: HRMS of the probe (MCMP)

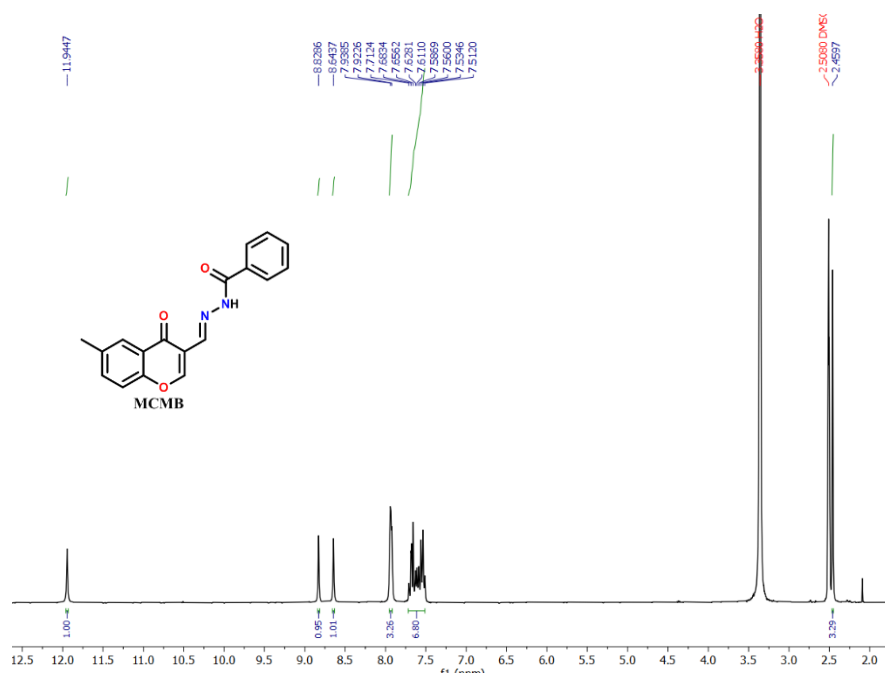


Figure S7: ¹H NMR (300 MHz) spectra of the probe (MCMB) in DMSO-d₆

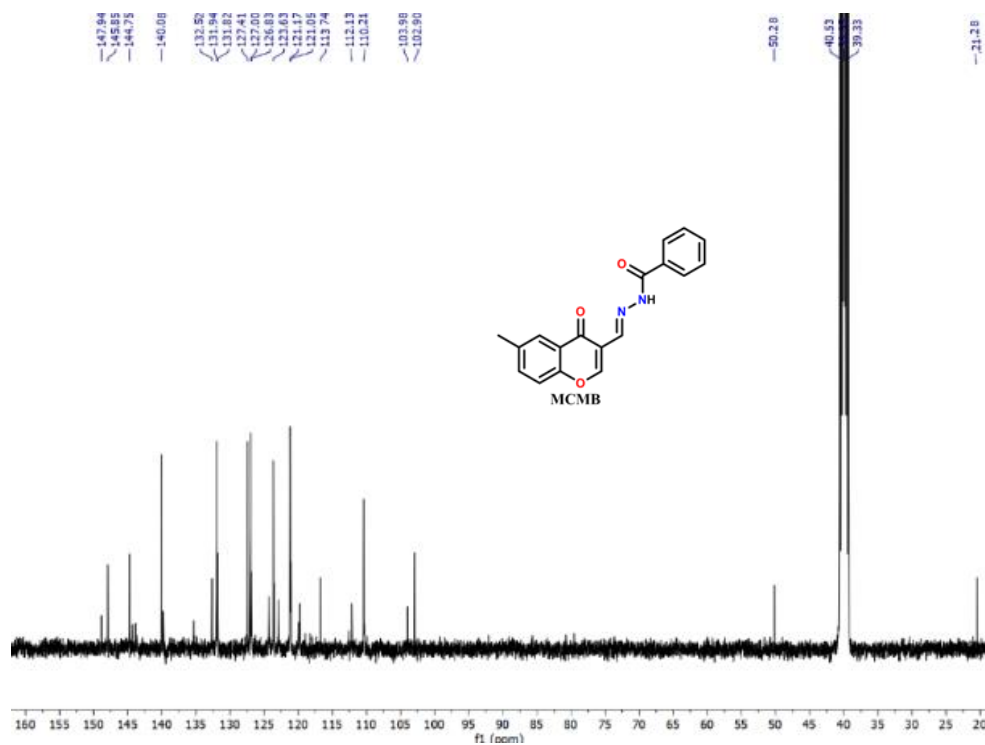


Figure S8: ¹³C NMR (75 MHz) spectra of the probe (MCMB) in DMSO-d₆

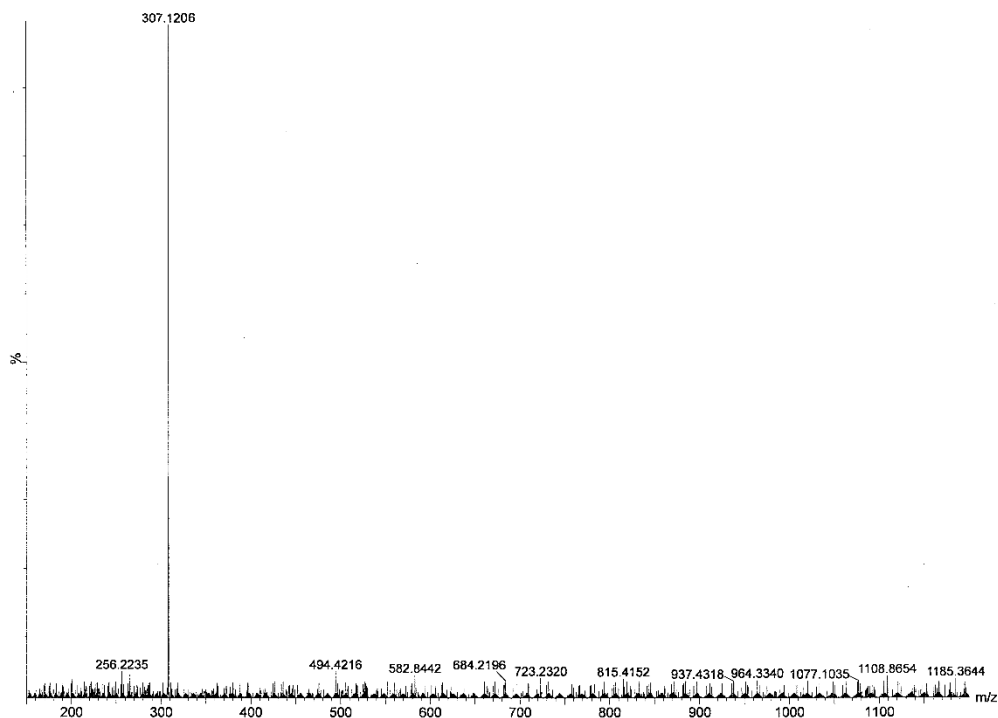


Figure S9: HRMS of the probe (MCMB)

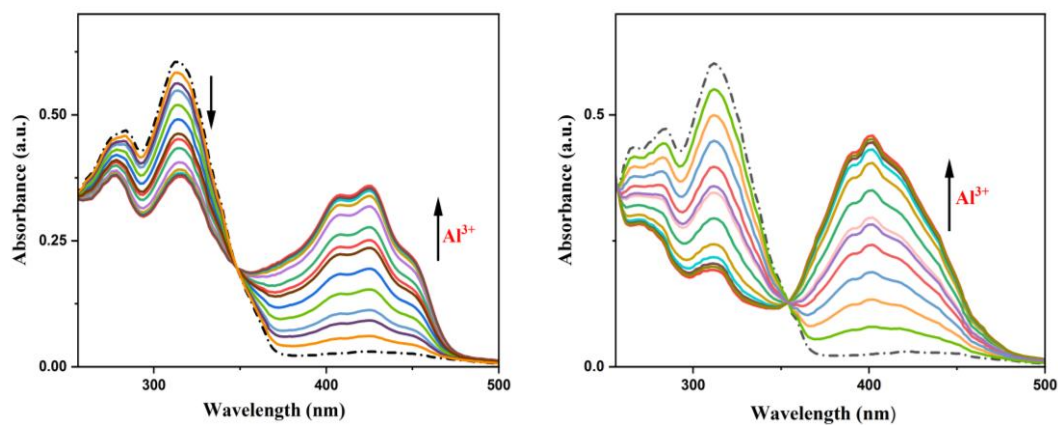


Figure S10: Change in UV-Vis spectrum of MCMP (10 μM) (Left side) and MCMB (10 μM) (Right side) upon incremental addition of Al^{3+} (0-20 μM) in MeOH / H_2O (9:1, v/v) (HEPES Buffer, pH =7.2) (left side) and change in UV-Vis spectrum of MCMB (10 μM) upon gradual addition of Al^{3+} (0-20 μM) in MeOH/ H_2O (9:1, v/v) (HEPES Buffer, pH =7.2) (right side).

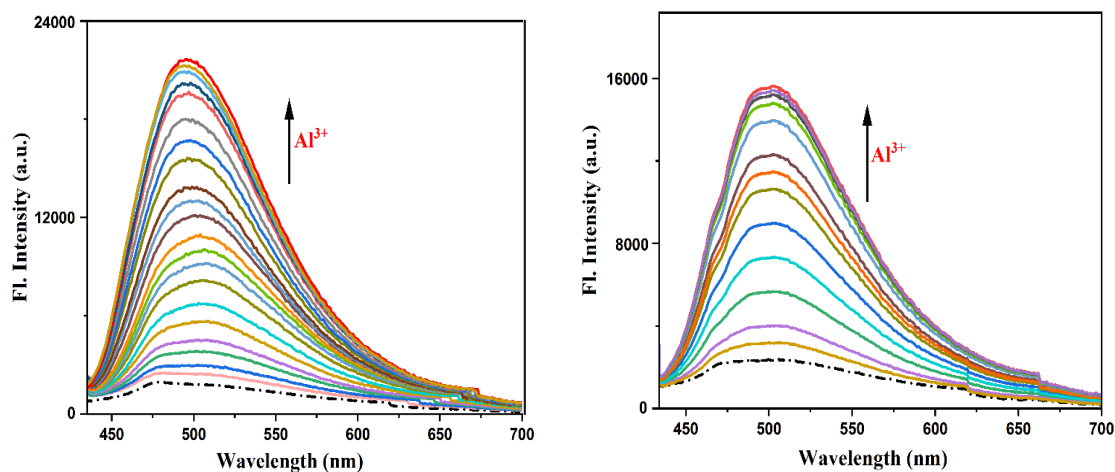


Figure S11: Change in emission intensity of MCMP (10 μM) (Left side) and MCMB (10 μM) (Right side) upon incremental addition of Al^{3+} ion (0-20 μM) in MeOH/ H_2O (9:1, v/v) (HEPES Buffer, pH =7.2).

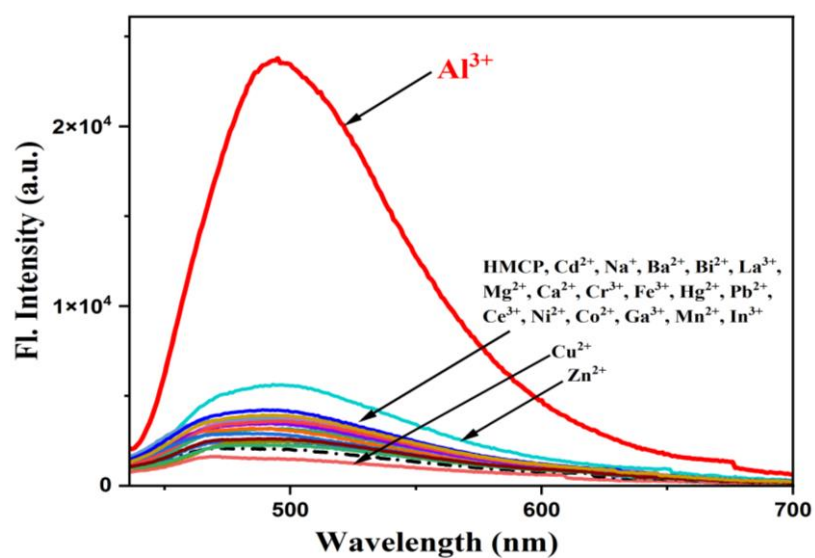


Figure S12: Change in emission intensity of HMCP (10 μM) upon addition of different metal ions (40 μM) in MeOH/ H_2O (9:1, v/v) (HEPES Buffer, pH =7.2).

Table S1: Fluorescence intensity enhancement of HMCP and its analogues (10 μM) upon addition of Al^{3+} (20 μM).

Compound	Emission intensity enhanced in presence of Al^{3+}	Excitation at respective isosbestic point
HMCP	~ 14 fold	351 nm
MCMP	~ 12 fold	347 nm
MCMB	~ 9 fold	354 nm

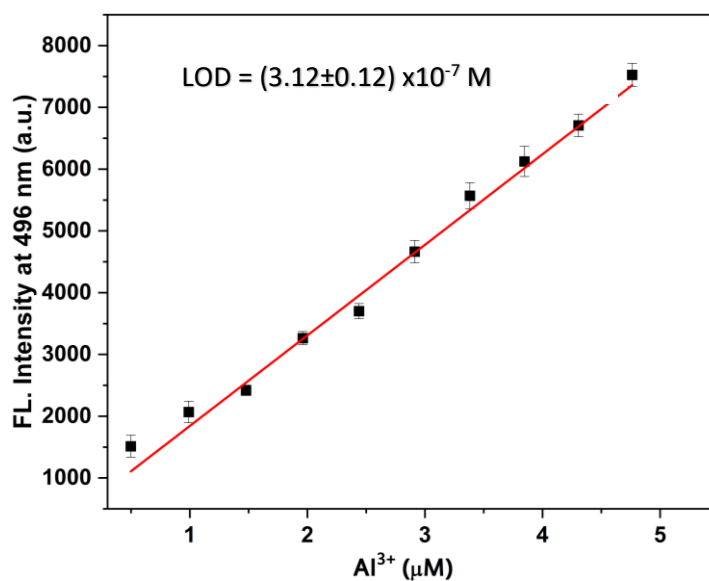


Figure S13: Linear response curve of HMCP at 496 nm depending on the Al^{3+} concentration

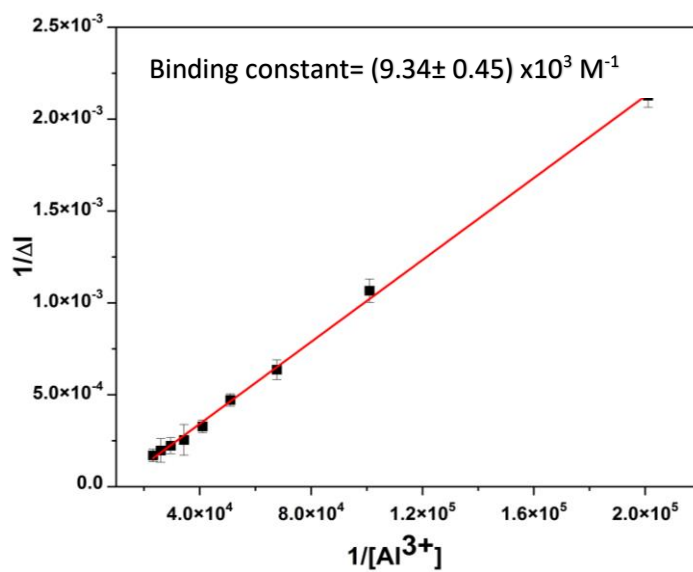


Figure S14: Determination of association constant of HMCP at 496 nm depending on the Al^{3+} concentration using Benesi-Hildebrand equation

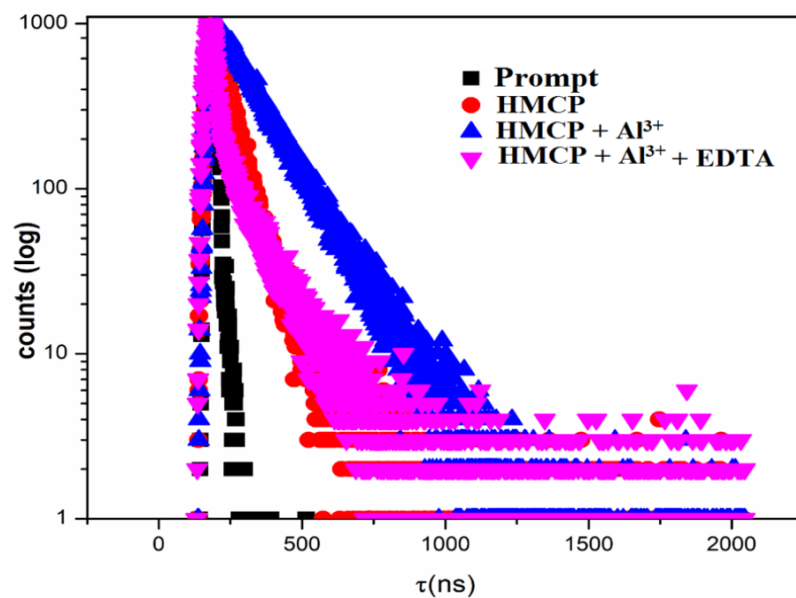


Figure S15: Lifetime decay profile of HMCP and HMCP-Al³⁺

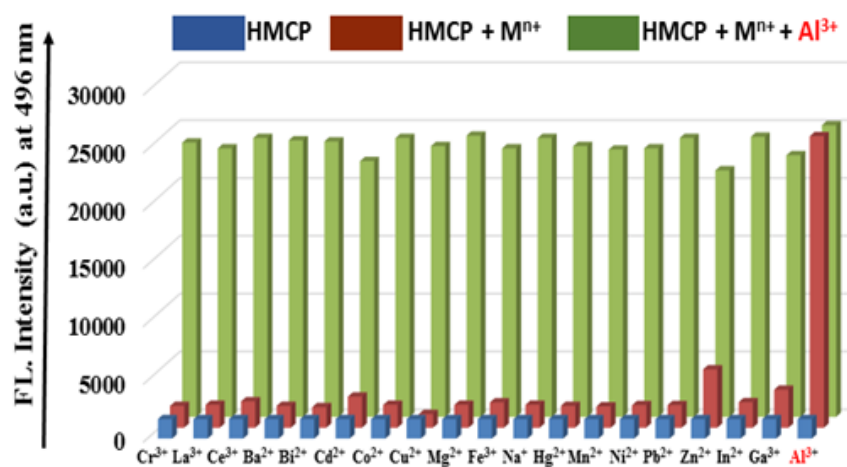


Figure S16: Bar diagram illustration of the relative emission intensity of HMCP upon addition of various metals (10 μM) in MeOH/H₂O (9:1, v/v) (HEPES Buffer, pH =7.2) (red bars) and Al³⁺ (20 μM) in presence of other metal ions (Green bars).

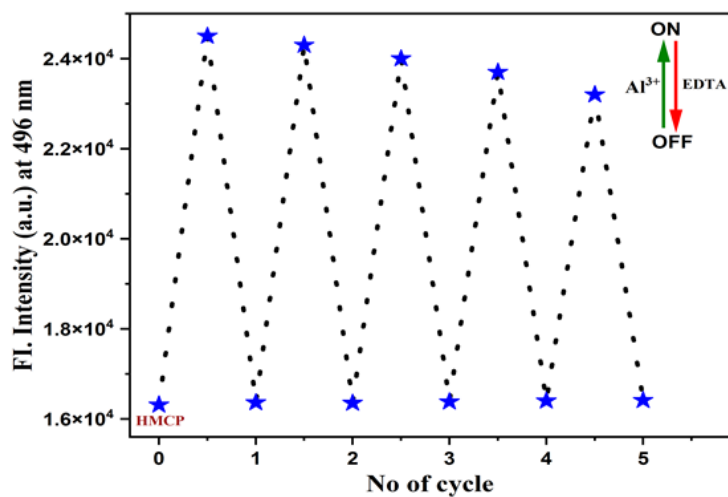


Figure S17: Fluorescence ‘OFF-ON-OFF’ repetitive cycle upon each sequential addition of Al³⁺ and EDTA ion for HMCP at 496 nm ($\lambda_{\text{ex}} = 351$ nm) in MeOH/H₂O (9:1, v/v) (HEPES Buffer, pH =7.2) solution

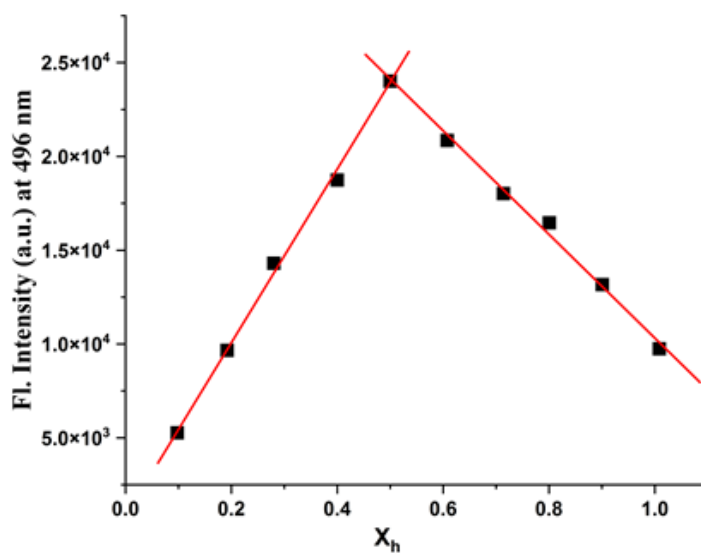


Figure S18: Job's plot of HMCP for Al³⁺

Table S2: Comparison of emission intensity enhancement of HMCP and its analogues upon addition of ct-DNA

Compound	Emission intensity enhanced by Al ³⁺	Emission intensity enhanced by DNA
HMCP	~ 14 fold	~ 8 fold
MCMP	~ 12 fold	~ 4.5 fold
MCMB	~ 9 fold	~ 1.6 fold

Table S3: Recovery experiment for various natural water samples using the proposed methods

Source	Water samples studied	Amount of standard Al ³⁺ spiked (μmol)	Total Al ³⁺ found (μmol) ^b	Recovery (%)
Tap water (Department of Chemistry)	Tap water 1	5	4.94 ± 0.04	98.8
	Tap water 2	10	9.95 ± 0.06	99.5
	Tap water 3	15	15.03 ± 0.35	100.2
Lake water (Jadavpur University campus)	Lake water 1	5	4.9 ± 0.07	98.6
	Lake water 2	10	9.65 ± 0.05	96.5
	Lake water 3	15	14.97 ± 0.06	99.8

^bRelative standard deviations were calculated based on three times of measurement.

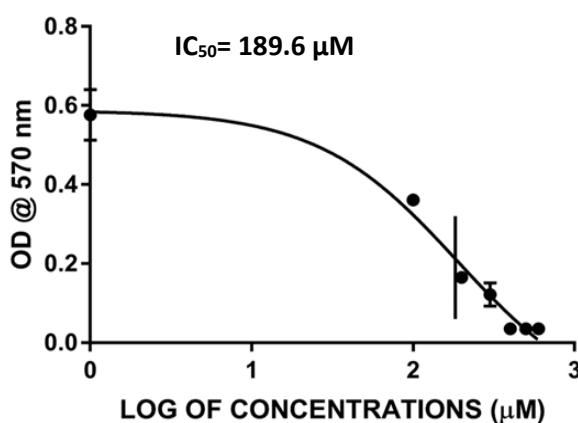


Figure S19: IC₅₀ dose of the probe (HMCP) in human breast cancer cells

Determination of fluorescence Quantum Yields (Φ) of HMCP and its complex with Al^{3+}

The luminescence quantum yield was determined using coumarin-153 as reference dye. The compounds and the reference dye were excited at the similar wavelength and the emission spectra were then studied. The area of the emission spectrum was integrated and the quantum yield is determined according to the following equation:

$$\phi_S/\phi_R = [A_S / A_R] \times [(Abs)_R / (Abs)_S] \times [n_S^2/n_R^2]$$

Here, ϕ_S and ϕ_R are the luminescence quantum yields of the sample and reference dye, respectively. A_S and A_R are the area under the emission spectra of the sample and the reference respectively, $(Abs)_S$ and $(Abs)_R$ are the respective optical densities of the sample and the reference solution at the wavelength of excitation, and n_S and n_R stand for the values of refractive index for the respective solvent used for the sample and reference.

The quantum yields of HMCP and HMCP- Al^{3+} are determined using the above mentioned equation and the values are found to be 0.03 and 0.21 respectively. Radiative rate constant K_r and total non radiative rate constant K_{nr} have been calculated using the equation $\tau^{-1} = K_r + K_{nr}$ and $K_r = \phi_f / \tau$ (Table. S4).

Table S4: Determination of Fluorescence life-time data, quantum yield, radiative and non-radiative rate constants

Compd.	Quantum yield(ϕ)	τ (ns)	$K_r(10^8 \times S^{-1})$	$K_{nr}(10^8 \times S^{-1})$
HMCP	0.03	1.12	0.2678	8.66
HMCP-Al^{3+}	0.21	4.24	0.4952	1.8632

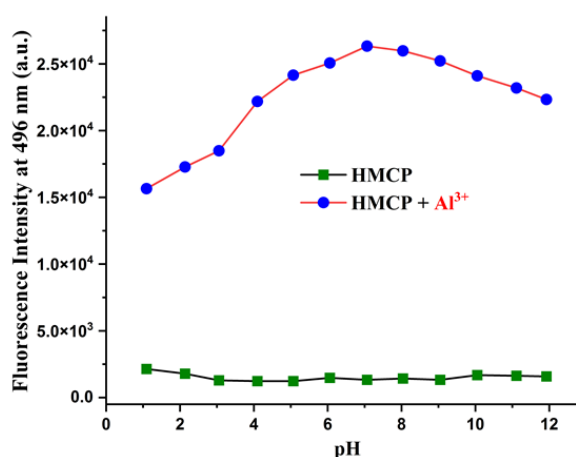


Figure S20: pH study of HMCP for Al^{3+}

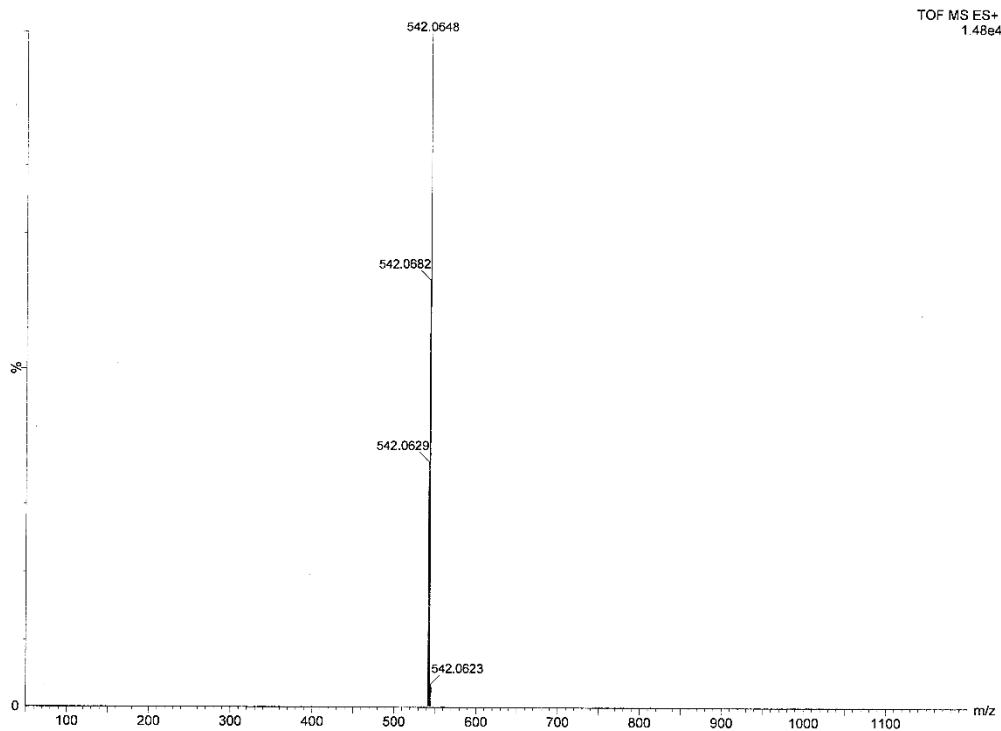


Figure S21: HRMS of HMCP-Al³⁺ complex

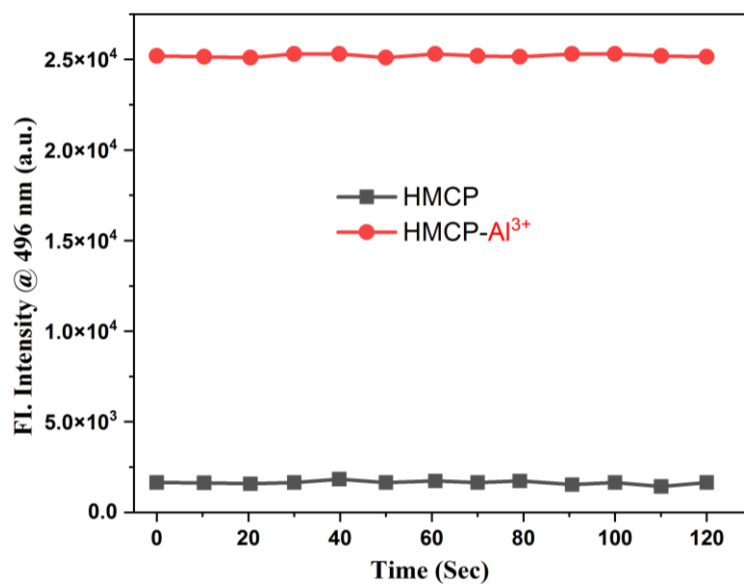


Fig. S22: Photosensitivity study of HMCP and its complex

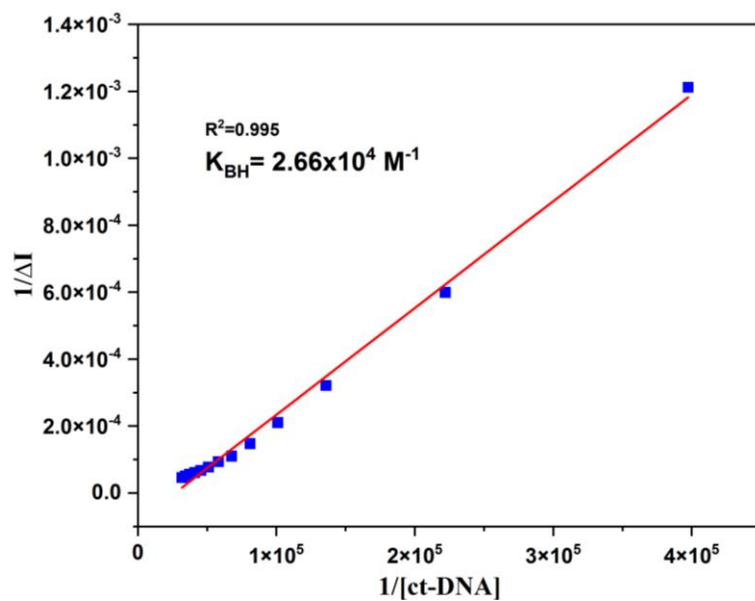


Fig. S23: Determination of binding constant of HMCP at 476 nm depending on ct-DNA concentration using Benesi-Hildebrand equation

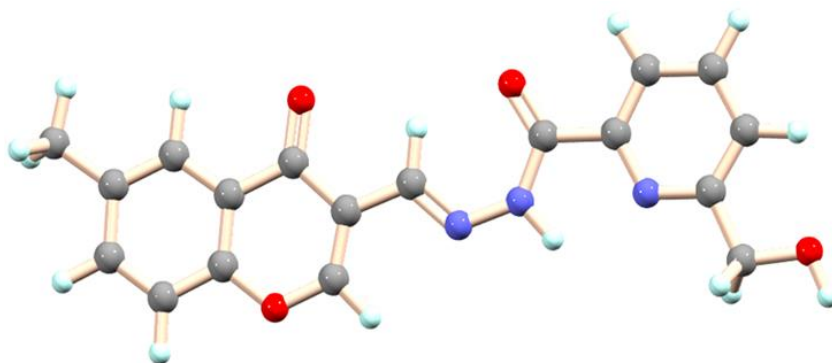


Figure S24: Optimized structure of HMCP calculated by DFT/B3LYP/6-31+G(d) method

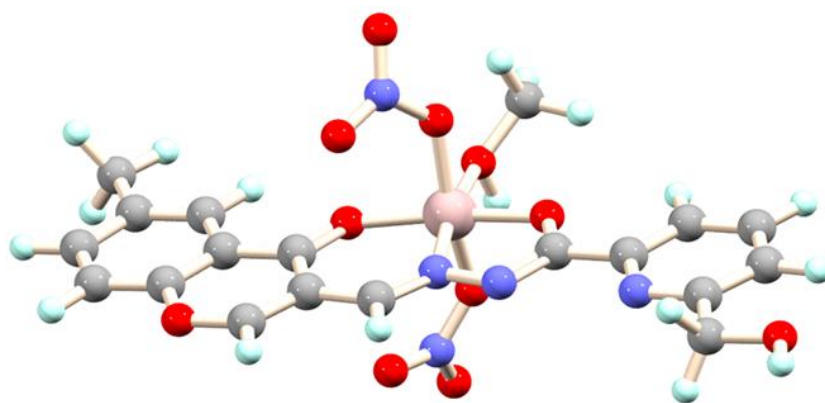


Figure S25. Optimized structure of HMCP-Al³⁺ complex calculated by DFT/B3LYP/6-31+G(d) method

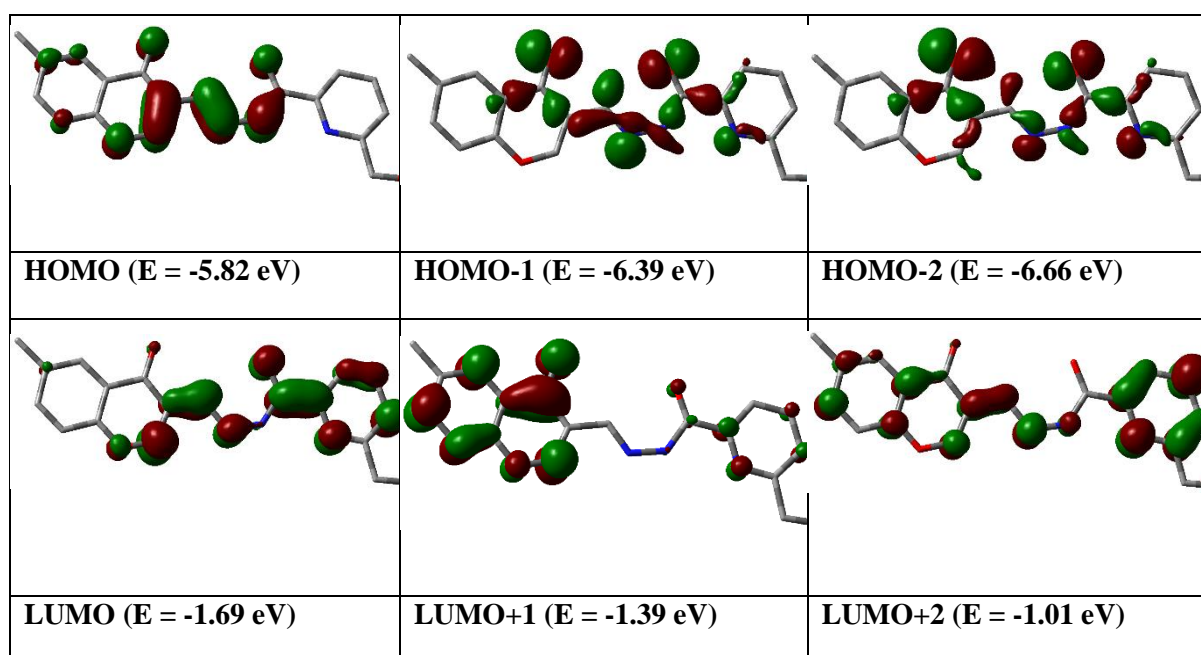


Figure S26. Contour plots of some selected molecular orbitals of HMCP

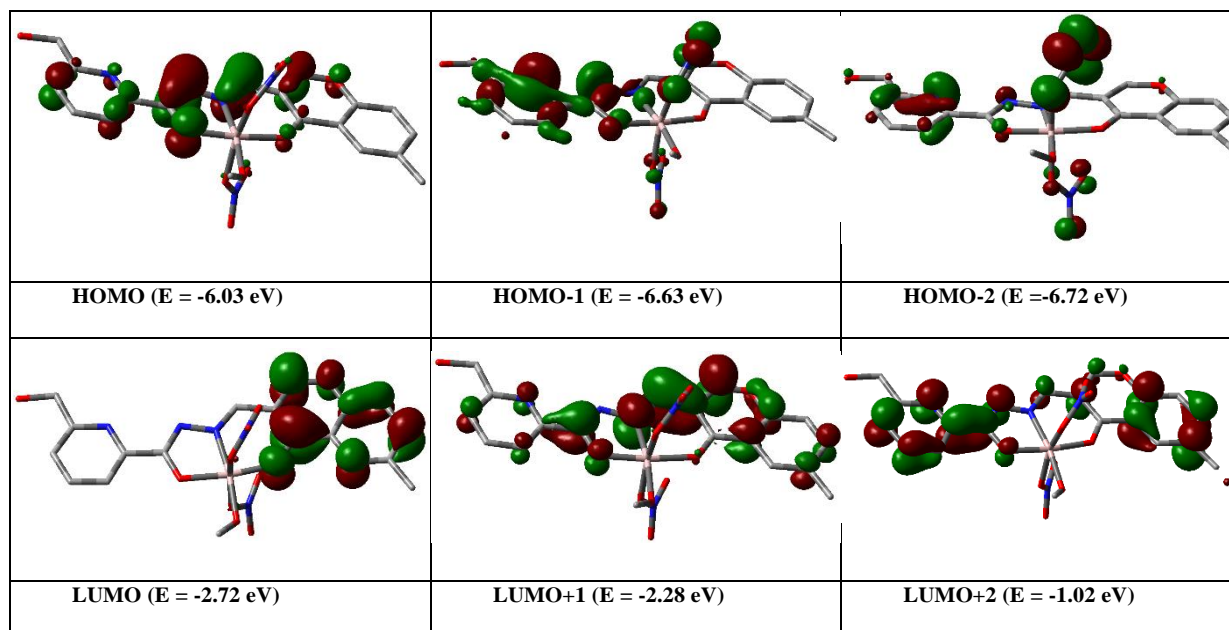


Figure S27. Contour plots of some selected molecular orbitals of HMCP-Al³⁺ complex

Table S5. Energy and compositions of some selected molecular orbitals of HMCP and HMCP-Al³⁺

MO	Energy (eV)	
	HMCP	HMCP-Al ³⁺
LUMO+5	0.74	-0.45
LUMO+4	0.02	-0.59
LUMO+3	-0.63	-0.73
LUMO+2	-1.01	-1.02
LUMO+1	-1.39	-2.28
LUMO	-1.69	-2.72

HOMO	-5.82	-6.03
HOMO-1	-6.39	-6.63
HOMO-2	-6.66	-6.72
HOMO-3	-6.69	-6.80
HOMO-4	-7.09	-6.85
HOMO-5	-7.13	-7.33

Table S6. Vertical electronic transitions calculated by TDDFT/B3LYP/CPCM method for HMCP and HMCP-Al³⁺ in methanol

Compounds	λ (nm)	E (eV)	Osc. Strength (f)	Key excitations	Character	$\lambda_{\text{expt.}}$ (nm) (ϵ , M ⁻¹ cm ⁻¹)
HMCP	335.44	3.6962	0.7610	(96%) HOMO→LUMO	$\pi \rightarrow \pi^*$	314 (60408)
	309.01	4.0124	0.0650	(91%) HOMO→LUMO+1	$\pi \rightarrow \pi^*$	283 (47192)
	277.95	4.4607	0.0637	(86%) HOMO→LUMO+2	$\pi \rightarrow \pi^*$	
HMCP-Al³⁺	380.93	3.2547	0.0868	(97%) HOMO→LUMO	$\pi \rightarrow \pi^*$	424 (61475)
	352.17	3.5206	0.8959	(96%) HOMO→LUMO+1	$\pi \rightarrow \pi^*$	407 (58289)
	310.88	3.9881	0.1218	(66%) HOMO-3→LUMO	$\pi \rightarrow \pi^*$	

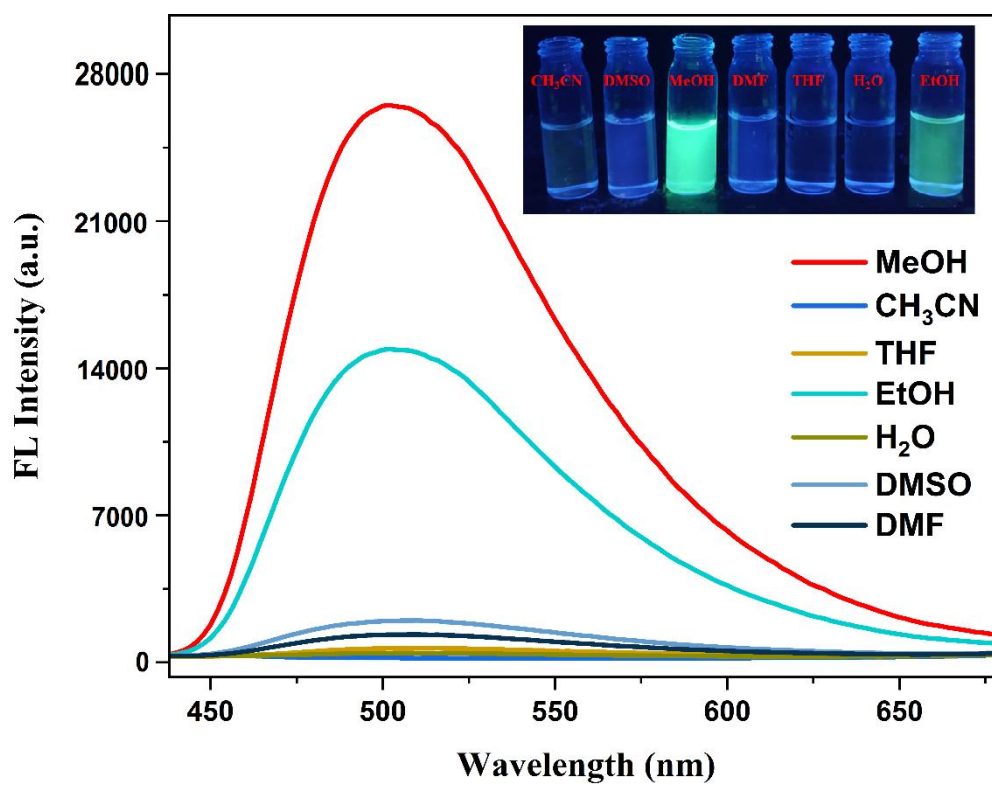
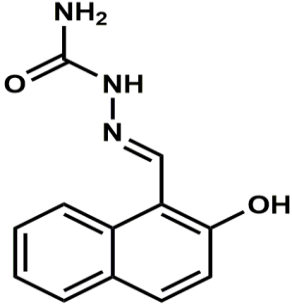
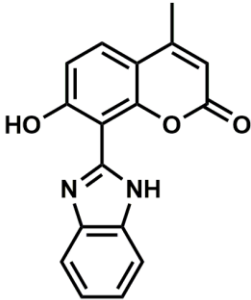
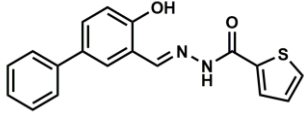
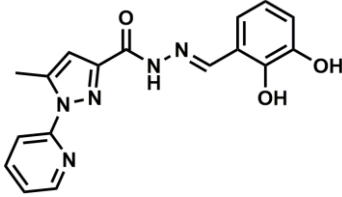
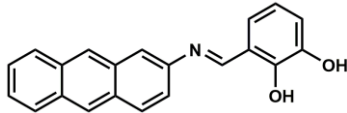
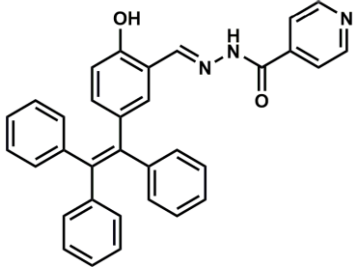
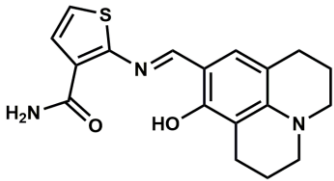
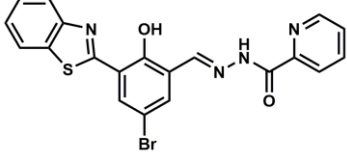
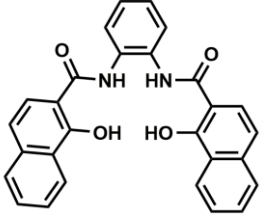
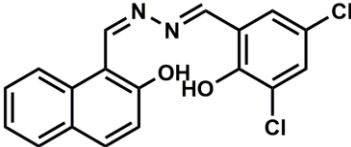
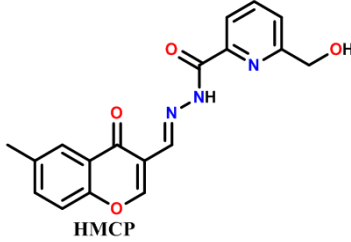


Figure S28: Solvent optimization: Emission intensity change and fluorescence image of HMCP (10 μ M) in different solvents in presence of Al³⁺ (20 μ M).

Table S7: Comparison of sensor HMCP with other previously reported probes with respect to testing condition LOD value and test strips experiment

Chemoreceptors	Testing Condition	Detection limit	Test Strips	References
	EtOH/H ₂ O, (1/9, v/v, pH=5.3, 25°C)	6.75x10 ⁻⁸ M	No	[1]
	ACN:H ₂ O (2:1, v/v, pH=7.2), HEPES Buffer	0.62 μM	No	[2]
	Acetonitrile-Water(4:1, v/v, pH=7.2)	0.5x10 ⁻⁹ M	Yes	[3]
	CH ₃ OH-H ₂ O (9:1, v/v)	4.78 μM	Yes	[4]
	H ₂ O	0.397 μM	No	[5]

	<p>MeOH-H₂O (9:1, v/v), Tris Buffer, pH=7.4</p>	<p>1.587x10⁻⁷ M</p>	<p>No</p>	<p>[6]</p>
	<p>MeCN-DMF (1:3, v/v)</p>	<p>1.4 μM</p>	<p>Yes</p>	<p>[7]</p>
	<p>H₂O-MeOH (1:1, v/v, pH=6.0)</p>	<p>31.2 nM</p>	<p>No</p>	<p>[8]</p>
	<p>DMF</p>	<p>5.0X10⁻⁶ M</p>	<p>No</p>	<p>[9]</p>
	<p>DMSO-H₂O (99:1, v/v, pH=7-8)</p>	<p>0.04 μM</p>	<p>No</p>	<p>[10]</p>
 <p>HMCP</p>	<p>MeOH/H₂O (9:1, v/v) (HEPES Buffer, pH=7.2)</p>	<p>3.12x10⁻⁷ M</p>	<p>Yes</p>	<p>Present Work</p>

References:

- 1 L. Hou, W. Liang, C. Deng, C. Zhang, B. Liu, S. Shuang and Y. Wang, *RSC Adv.*, 2020, **10**, 21629-21635
- 2 M. B. Maity, B. Dutta, A. Rahaman, N. Sahu, D. P. Mandal, S. Bhattacharjee and C. Sinha, *J. Mol. Struct.* 2022, **1250**, 131870
- 3 A. Biswas, R. Naskar, D. Mitra, A. Das, S. Gharami, N. Murmu and T. K. Mondal, *New J. Chem.*, 2022, **46**, 21968
- 4 B. Das, M. Dolai, A. Ghosh, A. Dhara, A. D. Mahapatra, D. Chattopadhyay, S. Mabhai, A. Jana, S. Dey and A. Misra, *Anal. Methods.*, 2021, **13**, 4266-4279
- 5 N. Mudi, M. Shyamal, P. K. Giri, S. S. Samanta and R. Ramirtz-Tagle and A. Misra, *J. Photochem. Photobiol.*, 2023, **22**, 1491-1503
- 6 M. Wang, L. Lu, W. Song, X. Wang, T. Sun, J. Zhu and J. Wang, *J. Lumin.*, 2021, **233**, 117911
- 7 J. S. Heo, D. Gil and C. Kim, *J. Fluoresc.*, 2022, **32**, 825-833
- 8 J. Wang, L. Feng, J. Chao, Y. Wang, S. Shuang, *Anal. Methods*, 2019, **11**, 5598
- 9 N. Ahfad, G. Mohammadnezhad, S. Meghdabi and H. Farrokhpour, *Spectrochim. Acta A Mol.*, 2020, **228**, 117753
- 10 J. A. Anshori, D. Ismalah, A. F. Abror, A. Zainuddin, I. W. Hidayat, M. Yusuf, R. Maharani, A. T. Hidayat, *RSC Adv.*, 2022, **12**, 2972